ioMosaic®
Minimizing risk. Maximizing potential.®

# Analysis of PRV Stability In Relief Systems Part IV:

*On the Estimation of Speed of Sound and Thermodynamic Properties for Fluid Flow and PRV Stability*

**An ioMosaic® Publication**

**G. A. Melhem, Ph.D., FAIChE**

IOMOSAIC® CORPORATION

# Analysis of PRV Stability In Relief Systems Part IV:
## On the Estimation of Speed of Sound and Thermodynamic Properties for Fluid Flow and PRV Stability

*Process Safety and Risk Management Practices*

authored by

G. A. Melhem, Ph.D., FAIChE

Printed October 18, 2024

**Notice:**

This document was prepared by ioMosaic® Corporation (**ioMosaic**) for Public Release. This document represents ioMosaic's best judgment in light of information available and researched prior to the time of publication.

Opinions in this document are based in part upon data and information available in the open literature, data developed or measured by ioMosaic, and/or information obtained from ioMosaic's advisors and affiliates. The reader is advised that ioMosaic has not independently verified all the data or the information contained therein. This document must be read in its entirety. The reader understands that no assurances can be made that all liabilities have been identified. This document does not constitute a legal opinion.

No person has been authorized by ioMosaic to provide any information or make any representation not contained in this document. Any use the reader makes of this document, or any reliance upon or decisions to be made based upon this document are the responsibility of the reader. ioMosaic does not accept any responsibility for damages, if any, suffered by the reader based upon this document.

**Revision Log:**

Revision 1: January 19, 2019
Revision 2: October 18, 2024

©ioMosaic Corporation ⇑ ⇓ All Rights Reserved Printed October 18, 2024

...

# Table of Contents

**1 Introduction** **5**

**2 How is Speed of Sound Calculated?** **5**

**3 Two Phase Speed of Sound** **6**

**4 Impact of Piping on Speed of Sound** **11**

**5 How is Speed of Sound Measured?** **13**

**6 Thermodynamic Properties** **15**

6.1 Isothermal Compressibility . . . . . 17

6.2 Isentropic Compressibility . . . . . 18

6.3 Volume Expansion Coefficient . . . . . 18

6.4 Pressure Rise Due to Thermal Expansion . . . . . 19

6.5 Isentropic Expansion Coefficient . . . . . 19

6.6 Joule-Thomson Coefficient . . . . . 19

6.7 Liquid Constant Volume Heat Capacity . . . . . 20

6.8 Bulk Modulus of Elasticity . . . . . 22

**7 Validation Data** **23**

7.1 Gases . . . . . 23

7.2 Liquids . . . . . 23

7.3 Two-Phase . . . . . 26

**8 Conclusions** **26**

**9 Appendix A - Ideal Gas Behavior** **27**

**10 Appendix B - Thermodynamics of Sonic Flow** **29**

©ioMosaic Corporation ⇑ ⇓ All Rights Reserved 

# List of Figures

1 Two-phase sonic velocity for propane as a function liquid holdup . . . . . 8
2 Calculated two phase speed of sound for air-water system at 20°C and 1 atm using Equation 11 . . . . . 9
3 Measured two phase speed of sound for air-water system at 20°C and 1.76 bara . . 10
4 Calculated critical line length as a function of vapor quality and twophase speed of sound [1] . . . . . 11
5 Sonic velocity as a function of tube wall modulus of elasticity . . . . . 13
6 Frequency resonance spectrum for liquid water and hydrazine in a quartz cell (open end, $L + 0.6d = 1$ cm) [2] . . . . . 14
7 Calculated inversion curve for Hydrogen . . . . . 20
8 Calculated vs. Measured Liquid Speed of Sound Data for n-alkanes at 1 atm . . . . 24
9 Calculated vs. Measured Liquid Speed of Sound Data for 1-alkenes at 1 atm . . . . 25
10 Calculated vs. Measured Liquid Speed of Sound Data for cycloalkanes at 1 atm . . 25
11 Predicted Error Bounds for Liquid Speed of Sound for Hydrocarbons using SuperChems . . . . . 26

©ioMosaic Corporation ⇑ ⇓ All Rights Reserved Printed October 18, 2024

# List of Tables

1 Propane properties at 293 K and 8.35 $\times 10^5$ Pa . . . . . 7
2 Calculated propane mixture maximum velocities . . . . . 7
3 Impact of piping flexibility on speed of sound reduction - Propane data at 293 K and 8.35 bara . . . . . 12
4 Selected Thermodynamic Properties Definitions . . . . . 16
5 Speed of Sound Estimates vs. Measured Data in m/s at 283 K . . . . . 23

©ioMosaic Corporation ⇑ ⇓ All Rights Reserved Printed October 18, 2024

# 1 Introduction

An independent and accurate estimation of the speed of sound can provide an important quality check for a multitude of single and multi-phase flow applications. More recently, proposed screening methods for the calculation of PRV stability require an accurate estimate of the speed of sound for the fluid/piping system. This paper outlines proper methods for the calculation of thermodynamic properties and speed of sound for single and multi-phase systems. Comparisons with actual measurements indicate that credible values can be obtained for single and multi-phase systems.

# 2 How is Speed of Sound Calculated?

The speed of sound, $c$, characterizes the propagation of an infinitesimal pressure wave in a fluid that is unconfined. The speed of sound can be calculated for a single or two-phase unconfined fluid by evaluating the change in mixture density (with or without slip) with respect to pressure. Where the effects of conduction heat transfer are negligible, the equilibrium speed of sound is given by the derivative of pressure with respect to density at isentropic (adiabatic) conditions:

$$c_s = \sqrt{\left(\frac{\partial P}{\partial \rho}\right)_s} = \sqrt{\frac{1}{\rho \kappa_s}} = \sqrt{\frac{C_p}{C_v}\frac{1}{\kappa_T \rho}} \tag{1}$$

where $\kappa_s$ is the isentropic compressibility, $\rho$ is the fluid mass density, $\kappa_T$ is the isothermal compressibility, $C_p$ is the real fluid heat capacity at constant pressure, $C_v$ is the real fluid heat capacity at constant volume, and $P$ is the system pressure.

Where the effects of conduction heat transfer are dominant, the frozen speed of sound is given by the derivative of pressure with respect to density at isothermal conditions:

$$c_T = \sqrt{\left(\frac{\partial P}{\partial \rho}\right)_T} = \sqrt{\frac{1}{\rho \kappa_T}} \tag{2}$$

The equilibrium (isentropic) speed of sound $c_s$ is always larger than the frozen (isothermal) speed of sound $c_T$:

$$\frac{c_s}{c_T} = \sqrt{\frac{C_p}{C_v}} \tag{3}$$

For most liquids (see later section on heat capacity ratio) and two phase flow, the heat capacity ratio is typically close to 1 and the change of pressure with respect to density at constant temperature is close to that at constant entropy at low to moderate pressures. As a result, the speed of sound for most liquids can be approximated by:

$$c_s^2 \simeq c_T^2 = \left[\frac{\partial P}{\partial \rho}\right]_T \tag{4}$$

For gases, the heat capacity ratio ranges typically from 1 to 1.4, and as a result the equilibrium speed of sound $c_s$ can be larger than the isothermal speed of sound, $c_T$, by as much as the $\sqrt{1.4}$ or 18 %.

Detailed methods for calculating single and two phase pipe flow, such as those used in SuperChems™ (a component of Process Safety Office® ), have an implicit built-in formulation of the speed of sound in the flow equations. Differential pipe flow solutions are used to calculate the axial profiles of temperature, pressure, velocity, composition, and density. Choke points, i.e. piping locations where the speed of sound is reached, depend intrinsically on pressure and density. In order for piping solutions to get the right choke conditions, both changes in pressure and density must be calculated accurately as a function of axial distance. Note that for two-phase slip equilibrium flow, the effective local liquid compositions at a specific axial distance are higher than the local equilibrium liquid compositions as calculated by most pipe flow methods.

# 3 Two Phase Speed of Sound

Using Equation 1, an expression for speed of sound of a two-phase mixture at constant composition can be obtained. The specific volume of the mixture, $\mathcal{V}_m = \frac{1}{\rho_m}$, is a function of the local vapor volume fraction accounting for slip / liquid holdup, $\epsilon_l = (1-\alpha)$:

$$\frac{1}{\mathcal{V}_m} = \frac{\epsilon_l}{\mathcal{V}_l} + \frac{1-\epsilon_l}{\mathcal{V}_g} \quad \text{or} \quad \rho_m = \alpha\rho_g + (1-\alpha)\rho_l \tag{5}$$

where $\alpha$ is the void fraction. $\epsilon_l$ is defined as a function of the slip ratio $u_g/u_l$ and the vapor mass fraction, $\mathcal{Y}$:

$$\frac{1}{\epsilon_l} = \frac{u_l}{u_g}\frac{\mathcal{Y}}{1-\mathcal{Y}}\frac{\mathcal{V}_g}{\mathcal{V}_l} + 1 \quad \text{or} \quad \frac{1}{1-\alpha} = \frac{u_l}{u_g}\frac{\mathcal{Y}}{1-\mathcal{Y}}\frac{\rho_l}{\rho_g} + 1 \tag{6}$$

where $u$ is the flow velocity. The speed of sound of the mixture is calculated by differentiating Equation 5 at constant entropy:

$$\left(\frac{\partial \frac{1}{\mathcal{V}_m}}{\partial P}\right)_s = -\frac{1}{\mathcal{V}_m^2}\left(\frac{\partial \mathcal{V}}{\partial P}\right)_s = \frac{1}{c_{m,s}^2} \quad \text{or} \quad \left(\frac{\partial \rho_m}{\partial P}\right)_s = \frac{1}{c_{m,s}^2} \tag{7}$$

Using the definition of $\epsilon_l$ and assuming constant mole fraction in both phases, Equation 7 becomes:

$$\frac{1}{c_{m,s}^2} = \frac{\epsilon_l}{c_{l,s}^2} + \frac{1-\epsilon_l}{c_{g,s}^2} + \frac{1}{\mathcal{V}_l}\frac{\partial \epsilon_l}{\partial P} - \frac{1}{\mathcal{V}_g}\frac{\partial \epsilon_l}{\partial P} \tag{8}$$

It can be shown that, after algebraic manipulations, Equation 7 for the calculation of sonic velocity of a two-phase mixture becomes:

$$\frac{1}{c_{m,s}^2} = \left[\frac{1-\epsilon_l}{\mathcal{V}_g} + \frac{\epsilon_l}{\mathcal{V}_l}\right]\left[\frac{\epsilon_l \mathcal{V}_l}{c_{l,s}^2} + \frac{(1-\epsilon_l)\mathcal{V}_g}{c_{g,s}^2}\right] \tag{9}$$

Table 1: Propane properties at 293 K and 8.35 $\times 10^5$ Pa

| Property | Liquid | Vapor |
|---|---|---|
| $\rho$, kg/m$^3$ | 523 | 18.1 |
| $\kappa$, Pa$^{-1}$ | 9.18 $\times 10^{-9}$ | 1.47 $\times 10^{-6}$ |
| $\beta$, K$^{-1}$ | 0.00408 | 0.00558 |
| $c_s$, m/s | 733 | 218 |

Table 2: Calculated propane mixture maximum velocities

| $\epsilon_l$ | $c_{m,s}$ in (m/s) | $\epsilon_l$ | $c_{m,s}$ in (m/s) |
|---|---|---|---|
| 0.00 | 218 | 0.60 | 81.7 |
| 0.05 | 145 | 0.70 | 87.6 |
| 0.10 | 118 | 0.80 | 100 |
| 0.20 | 95 | 0.90 | 133 |
| 0.30 | 85.1 | 0.95 | 181 |
| 0.40 | 80.7 | 0.99 | 357 |
| 0.50 | 79.7 | 1.00 | 732 |

This derivation is consistent with the one reported by Wallis [3] for a homogeneous two-phase mixture where the vapor quality does not change, i.e. frozen. For flashing flow, the use of Equation 1 is required with an appropriate expression for mixture density as a function of flash fraction or vapor quality or void fraction. If we express the mixture density as a function of void fraction, $\alpha = 1 - \epsilon_l$:

$$\rho_m = \alpha\rho_g + (1-\alpha)\rho_l \tag{10}$$

We can calculate the mixture two-phase speed of sound in a similar fashion to Equation 9:

$$c_{m,s}^2 = \frac{1}{\frac{\alpha}{c_{g,s}^2} + \frac{1-\alpha}{c_{l,s}^2} + (\rho_g - \rho_l)\left[\frac{\partial\alpha}{\partial P}\right]_s} \tag{11}$$

Note that $\frac{\partial\alpha}{\partial P}$ is always negative. As a result, the two phase speed of sound for flashing flow is always less than that for frozen flow (void fraction does not change).

As an illustration, we calculate the speed of sound in a mixture of saturated propane at 293 K for values of $\epsilon_l$ ranging from 0 to 1. Table 1 shows calculated properties for saturated propane at 293 K using the Melhem modification of the Peng-Robinson equation of state as implemented in SuperChems.

Substituting these values in Equation 9 yield the maximum velocities summarized in Table 2 and

Figure 1: Two-phase sonic velocity for propane as a function liquid holdup

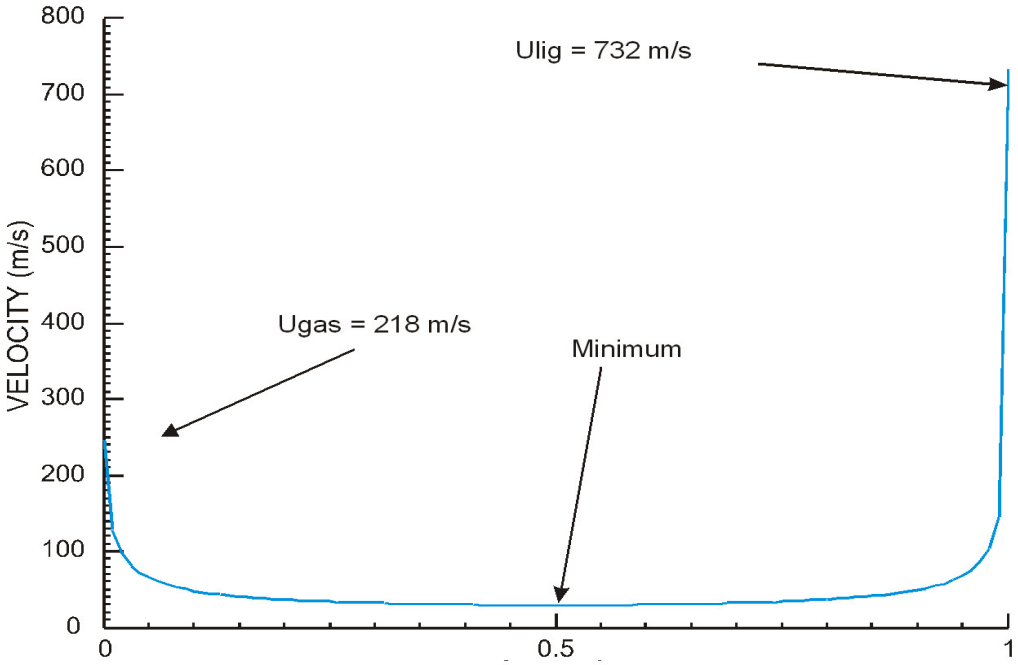


Figure 1. It is interesting to note that the mixture maximum velocity exhibits a minimum at an $\epsilon_l$ value of 1/2. This is caused by the mixture having a density close to that of the liquid and a compressibility close to that of the gas. At an $\epsilon_l$ value of 1/2, the two-phase mixture will have a void fraction of 1/2 (vapor mass fraction of 0.035).

The speed of sound values used in the estimation of pressure wave travel time can be subject to uncertainty. This is most important for liquids and two-phase systems. The presence of small amounts of entrained gas in liquids can reduce the speed of sound. Adding a small amount of gas to a liquid, say 0.01 % by weight can lower the speed of sound for the two-phase mixture by as much as a factor of two. Note that the two-phase speed of sound depends on the change of vapor quality (flash fraction) with pressure, temperature, and composition. Flashing flow speed of sound values can be as low as 10 or 15 m/s. We can calculate the two-phase mixture velocity for flashing flow using Equation 11:

$$\begin{aligned}
\frac{\alpha}{c_{g,s}^2} &= \frac{0.50}{218^2} = 1.052 \times 10^{-5} \\
\frac{1-\alpha}{c_{l,s}^2} &= \frac{0.50}{733^2} = 0.930 \times 10^{-6} \\
(\rho_g - \rho_l)\left[\frac{\partial \alpha}{\partial P}\right]_s &= (18.1 - 523) \times -2.747 \times 10^{-6} = 0.00138
\end{aligned}$$

We calculate a value of 26.8 m/s:

$$c_{m,s} = \sqrt{\frac{1}{1.052 \times 10^{-5} + 0.93 \times 10^{-6} + 0.00138}} = 26.8 \text{ m/s} \tag{12}$$

Note the significant impact of the $(\rho_g - \rho_l)\left[\frac{\partial \alpha}{\partial P}\right]_s$ term on the final value of $c_{m,s}$. When the pressure drops below the bubble point for liquid flow, the acoustic velocities will be reduced significantly due to flashing. If phase change occurs during the passage of a pressure wave, then the wave speed will depend on the degree to which equilibrium is reached.

For frozen systems, i.e. non-flashing systems where the vapor quality does not change with pressure such as air-water ($\frac{\partial \alpha}{\partial P} \ll 0$), we can show that small amounts of dissolved air can have a significant impact on the homogeneous two phase speed of sound. This is shown in Figure 2 for air-water at 20°C and 1 atmosphere. Note the speed of sound of the air-water mixture is reduced from 1475 m/s for water without dissolved air to 1000 m/s for water with 100 ppmw of dissolved air. This is because 100 ppmw of dissolved air translates into 7.7 volume % air as shown by Figure 2. The calculated mixture speed of sound shown in Figure 2 is in excellent agreement with actual measured values reported by Henry et al. [4] as shown in Figure 3. More recently, Hos et al. [5] reported an effective speed of sound for the water/piping system used in testing PRV stability for liquid water of 857 m/s. This lower value is mostly due to the impact of dissolved air in water and is substantially lower than 1475 m/s.

Figure 2: Calculated two phase speed of sound for air-water system at 20°C and 1 atm using Equation 11

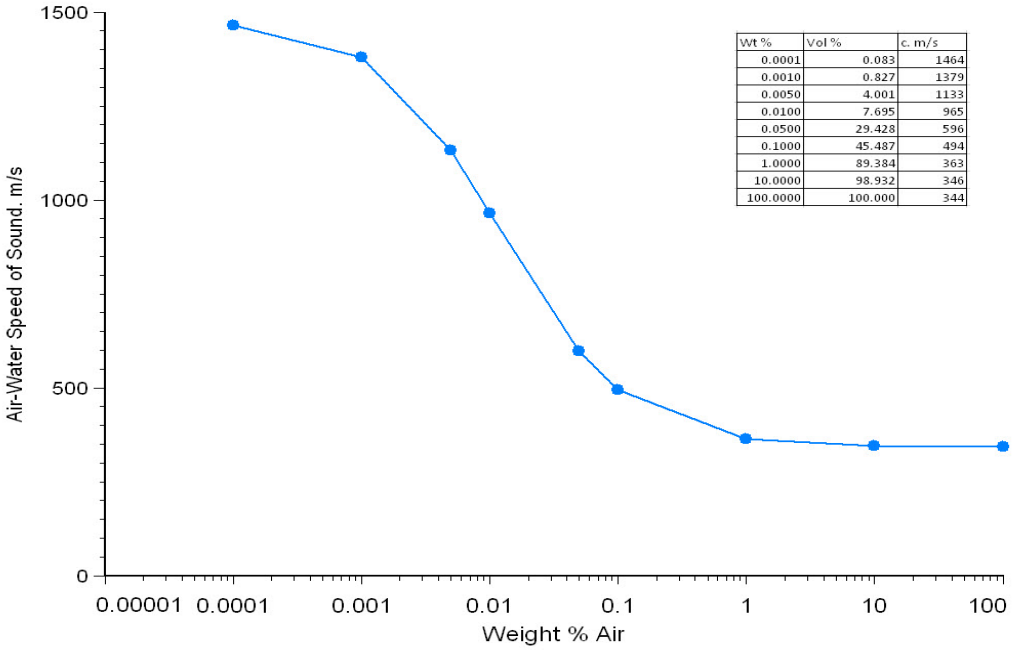


The above equations for two phase speed of sound are applicable to a homogeneous mixture of liquid and vapor. For other two phase flow regimes, such as stratified flow for example, a single mixture speed of sound value does not exist as each of the phases flows continuously in the flow direction. Equation 11 can be used to estimate the mixture two-phase speed of sound for slug flow as long as one assumes that the slugs are idealized, i.e. each liquid slug occupies the entire pipe flow area and has a certain length. In this case the void faction is calculated by dividing the length of pipe occupied by vapor by the total pipe length.

Figure 3: Measured two phase speed of sound for air-water system at 20°C and 1.76 bara

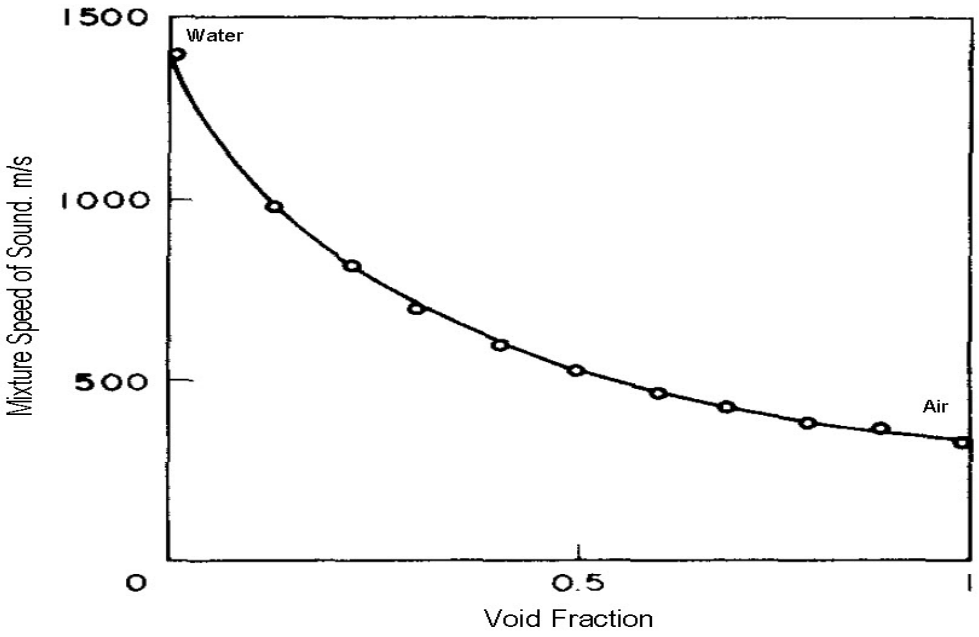


Hos [1] recently demonstrated using one dimensional fluid dynamics that the mixture speed of sound is by far the most crucial parameter influencing pressure relief valve stability. The critical line length [6] tends to zero at very low mixture speed of sound values as illustrated in Figure 4.

Oil-water systems are common in refining and exploration. The mixture density can be expressed similarly to Equation 10:

$$\rho_m = \alpha\rho_g + (1-\alpha)\left[\beta\rho_w + (1-\beta)\rho_o\right] \tag{13}$$

where $\beta$ is the volumetric fraction of water in the oil-water mixture, $\rho_w$ is the water density and $\rho_o$ is the oil density.

Several correlations based on test data exist for the estimation of speed of sound in oil without dissolved gas (dead oil) such as the correlation by Batzle and Wang:

$$c = \frac{15450}{\sqrt{77.1 + API}} - 3.7T + 4.64P + 0.0115\left(0.36\sqrt{API - 1}\right)TP \tag{14}$$

where $c$ is the speed of sound in m/s, $P$ is pressure in MPa, T is temperature in C, and $API$ is the API gravity number given by:

$$API = \frac{141.5}{\rho} - 131.5 \tag{15}$$

where $\rho$ is the liquid density in $\mathrm{g/cm^3}$ at 15.6 C and atmospheric pressure. Water has an API gravity number of 10.

Figure 4: Calculated critical line length as a function of vapor quality and twophase speed of sound [1]

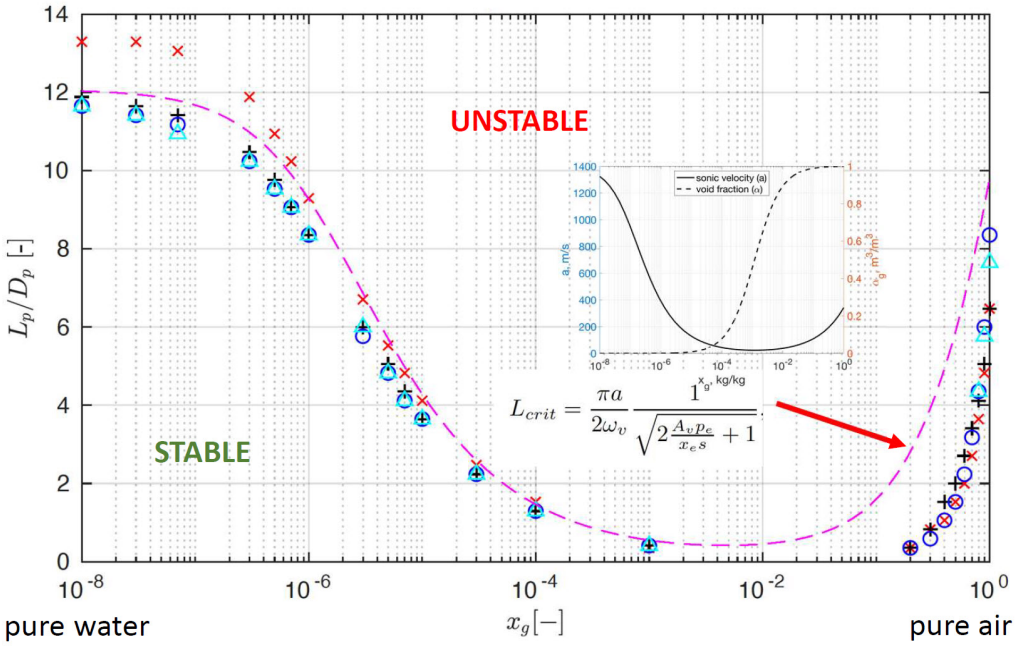


# 4 Impact of Piping on Speed of Sound

Piping flexibility can lower the value of the speed of sound. This occurs because pipes are not infinitely rigid and they will bulge or expand slightly under the influence of high pressure. This is equivalent to the fluid being more compressible, and as a result the speed of sound is reduced. The effective speed of sound, $c_e$, of a fluid confined by an elastic tube wall depends on both the fluid properties and the pipe elasticity. For rigid piping, the speed of sound is equal to the fluid speed of sound:

$$c_e = c_s = \sqrt{\frac{1}{\kappa_s \rho}} = \sqrt{\left[\frac{\partial P}{\partial \rho}\right]_s} = \sqrt{\frac{C_p}{C_v}\frac{1}{\kappa_T \rho}} = \sqrt{\frac{C_p}{C_v}\left[\frac{\partial P}{\partial \rho}\right]_T} \tag{16}$$

For piping that is anchored against longitudinal movement throughout its length:

$$c_e = c_s \eta = c_s \frac{1}{\sqrt{1 + \frac{E_f}{E_{solid}}\frac{d}{\delta}(1-\nu^2)}} \tag{17}$$

Where $E_f$ is the fluid adiabatic bulk modulus of elasticity [1], $E_{solid}$ is the pipe material of construction modulus of elasticity, $d/\delta$ is the piping diameter to thickness ratio, and $\nu$ is Poisson's ratio ($\simeq 0.3$). An equation of state is typically used to calculate the fluid compressibility factors since this data is not readily available for all fluids and especially for mixtures.

[1] $E_f = \frac{1}{\frac{C_v}{C_p}\kappa_T} = \frac{C_p}{C_v}\frac{1}{\kappa_T} = \frac{C_p}{C_v}E_T$. The isothermal bulk modulus of elasticity is also used for liquids assuming the liquid heat capacity ratio is 1 which is not always a good assumption for all liquids. $E_f = \frac{1}{\kappa_T}$

Table 3: Impact of piping flexibility on speed of sound reduction - Propane data at 293 K and 8.35 bara

| Material | Piping Schedule US | $E_f$, GPa | $\frac{d}{\delta}$ | $\eta$ |
|---|---|---|---|---|
| Liquid Water | 5 | 2.19 | 52.2 | 0.799 |
| Liquid Water | 10 | 2.19 | 35.5 | 0.850 |
| Liquid Water | 40 | 2.19 | 13.4 | 0.934 |
| Liquid Water | 80 | 2.19 | 11.3 | 0.944 |
| Liquid Water | 160 | 2.19 | 6.47 | 0.967 |
| Liquid Propane | 5 | 0.11 | 52.2 | 0.986 |
| Liquid Propane | 10 | 0.11 | 35.5 | 0.991 |
| Liquid Propane | 40 | 0.11 | 13.4 | 0.996 |
| Liquid Propane | 80 | 0.11 | 11.3 | 0.997 |
| Liquid Propane | 160 | 0.11 | 6.47 | 0.998 |
| Vapor Propane | 5 | $6.8\times10^{-4}$ | 52.2 | 1.000 |
| Vapor Propane | 10 | $6.8\times10^{-4}$ | 35.5 | 1.000 |
| Vapor Propane | 40 | $6.8\times10^{-4}$ | 13.4 | 1.000 |
| Vapor Propane | 80 | $6.8\times10^{-4}$ | 11.3 | 1.000 |
| Vapor Propane | 160 | $6.8\times10^{-4}$ | 6.47 | 1.000 |

For piping anchored against longitudinal movement at the upper end:

$$c_e = c_s\eta = c_s\frac{1}{\sqrt{1+\frac{E_f}{E_{solid}}\frac{d}{\delta}\left(1.25-\nu\right)}} \tag{18}$$

For piping where frequent expansion joints are present:

$$c_e = c_s\eta = c_s\frac{1}{\sqrt{1+\underbrace{\frac{E_f}{E_{solid}}\frac{d}{\delta}}_{\beta}}} \tag{19}$$

The impact of piping flexibility on speed of sound estimates is illustrated in Table 3 for steel piping with frequent expansion joints. The speed of sound reduction is most important for liquids that are highly incompressible, such as water, where thin wall piping is used.

The various equations used above for the effective speed of sound $c_e$ are typically expressed in one form as shown by Equation 19 because the values of $1-\nu^2$ and $1.25-\nu$ are approximately one. As the value of $\beta = \frac{E_f}{E_{solid}}\frac{d}{\delta}$ tends towards a value of 10, the ratio of $\eta = \frac{c_e}{c_s}$ tends towards 0.3 as shown in Figure 5.

The ratio of $\frac{E_f}{E_{solid}}$ can also be expressed in terms of density and speed of sound (see Table 4):

$$\frac{E_f}{E_{solid}} = \left(\frac{c_s}{c_{s,solid}}\right)^2\frac{\rho}{\rho_{solid}} \tag{20}$$

Figure 5: Sonic velocity as a function of tube wall modulus of elasticity

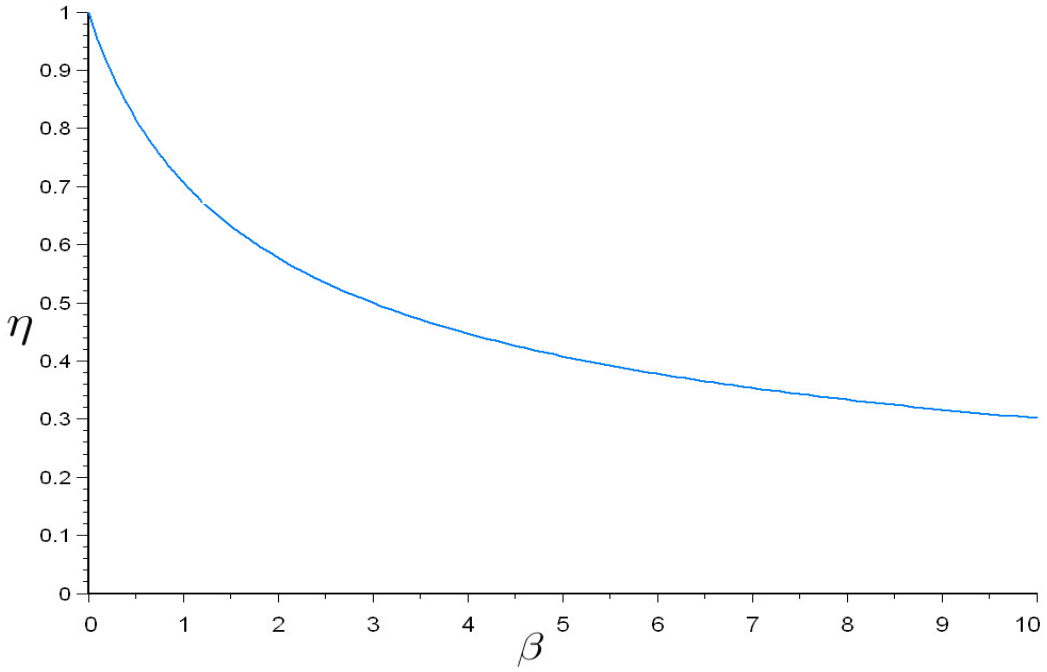


In general the following equation can be used with reasonable accuracy regardless for all piping configurations:

$$\boxed{c_e = c_s \eta = c_s \frac{1}{\sqrt{1 + \frac{E_f}{E_{solid}} \frac{d}{\delta}}} = c_s \frac{1}{\sqrt{1 + \left(\frac{c_s}{c_{s,solid}}\right)^2 \left(\frac{\rho}{\rho_{solid}}\right) \left(\frac{d}{\delta}\right)}}} \tag{21}$$

As long as the wall thickness is at least 1 % of the diameter (thick pipe), or the pipe is rigid, then the motion of the tube wall does not influence the wave propagation speed of the fluid for all commercial steel pipe and tubing components.

# 5 How is Speed of Sound Measured?

The speed of sound in a fluid is typically measured using resonance. Sound is the speed of transmission of a small disturbance (pressure wave) through a medium (gas, liquid, or solid). Sound cannot travel through vacuum. Resonance occurs when one object is vibrating at the same natural frequency of another object which forces the other object into vibration. Resonance can also occur from standing waves. A standing wave is created when two waves traveling in opposite directions interfere with each other and produce a large amplitude wave (see Figure 6).

To measure the speed of sound of a fluid, a pipe with a closed end is used. A sound wave is created which travels down the pipe. As the sound wave is reflected and returns to the open end, interference between the two sound waves occurs. If the length of the closed end pipe is 1/4th of

a wavelength, then a standing wave is created and resonance occurs. The velocity of sound is then calculated from:

$$c = 4\,(L + 0.3d)\,f \tag{22}$$

where $L$ is the length of the pipe/tube with a closed end, $d$ is the inside diameter of the pipe/tube, and $f$ is the frequency of the source generating the sound wave such a tuning fork for example. If the pipe end is open then:

$$c = 2\,(L + 0.6d)\,f \tag{23}$$

Figure 6: Frequency resonance spectrum for liquid water and hydrazine in a quartz cell (open end, $L + 0.6d = 1$ cm) [2]

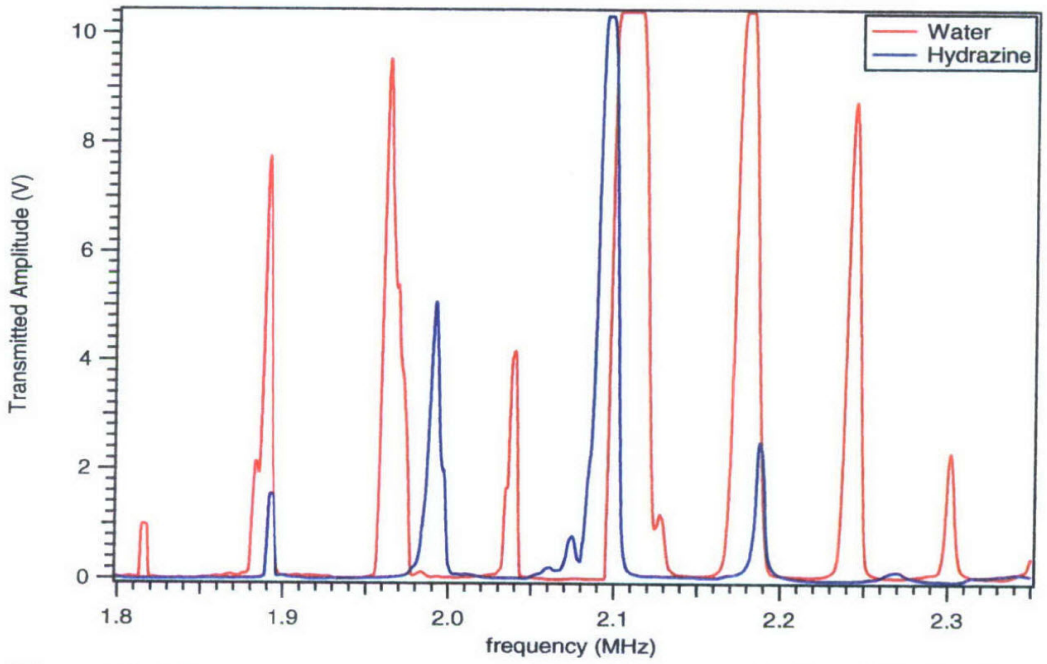


Figure 6 shows measured resonance frequency spectrum for liquid water and hydrazine. Using the second and third frequency peaks for water and hydrazine we calculate a speed of sound of:

$$\begin{aligned} c_{H_2O} &= 2 \times 1 \times (1.96 - 1.89) \times 10^6 = 140000 \text{ cm/s } \textit{or } 1400 \text{ m/s} \\ c_{H_4N_2} &= 2 \times 1 \times (1.99 - 1.89) \times 10^6 = 200000 \text{ cm/s } \textit{or } 2000 \text{ m/s} \end{aligned}$$

The liquid resonance frequency difference varies from peak to peak due to interference from the cell walls. As a result, an average of several frequency differences is used to calculate the actual speed of sound. The reported measured speed of sound of water is 1483 m/s and for hydrazine is 2083 m/s. Other data reported by the same reference included methanol (1109 m/s), 2-propanol (1181 m/s), acetone (1208 m/s), and tetrachloromethane (938 m/s).

# 6 Thermodynamic Properties

Table 4 provides definitions for common thermodynamic properties often used in the calculation of fluid flow, phase behavior, and phase equilibrium. The partial derivatives of thermodynamic properties necessary for equilibrium, and fluid flow calculations can be calculated as a function of temperature, pressure, and change in composition. An equation of state is required in order to fully develop these thermodynamic relationships.

For two-phase systems, the vapor and liquid phases are considered to be homogeneous in composition and state. When a change of phase is exhibited, mass may be transferred from one phase to another. Thus the state of either phase may be altered by a change in composition, temperature, or pressure. The value of any thermodynamic property, $\theta$, in either phase may be expressed in the form:

$$\theta = f(T, P, n_1, n_2, \cdots, n_C) \tag{24}$$

We can write an equation for a change in property $M$ during a small change in phase:

$$d\theta = \left(\frac{\partial\theta}{\partial P}\right)_{T,n_1,n_2,\cdots} dP + \left(\frac{\partial\theta}{\partial T}\right)_{P,n_1,n_2,\cdots} dT + \sum_i^C \left(\frac{\partial\theta}{\partial n_i}\right)_{T,P,n_{j\neq i}} dn_i \tag{25}$$

This differential statement of Equation 24 is extended to permit calculation of the change of property, $M$, with respect to any other system variable, such as time for example:

$$\frac{d\theta}{dt} = \left(\frac{\partial\theta}{\partial P}\right)_{T,n_1,n_2,\cdots} \frac{dP}{dt} + \left(\frac{\partial\theta}{\partial T}\right)_{P,n_1,n_2,\cdots} \frac{dT}{dt} + \sum_i^C \left(\frac{\partial\theta}{\partial n_i}\right)_{T,P,n_{j\neq i}} \frac{dn_i}{dt} \tag{26}$$

It is also useful in fluid flow to express thermodynamic properties as a function of system variables such as pressure and density. Such expressions are useful in the development of boundary conditions for example for one dimensional flow. If we assume no change in composition, we can develop the following relationships for temperature, specific internal energy, specific enthalpy, and specific entropy as a function of pressure and density:

$$\frac{dT}{dt} = \left(\frac{\partial T}{\partial P}\right)_\rho \frac{dP}{dt} + \left(\frac{\partial T}{\partial \rho}\right)_P \frac{d\rho}{dt} = \underbrace{\left(\frac{\beta T}{\rho C_p} + \frac{1}{\rho\beta c_s^2}\right)}_{\frac{\kappa_T}{\beta}} \frac{dP}{dt} - \left(\frac{1}{\beta\rho}\right)\frac{d\rho}{dt} \tag{27}$$

$$\frac{de}{dt} = \left(\frac{\partial e}{\partial P}\right)_\rho \frac{dP}{dt} + \left(\frac{\partial e}{\partial \rho}\right)_P \frac{d\rho}{dt} = \left(\frac{C_p}{\beta\rho c_s^2}\right)\frac{dP}{dt} + \left(\frac{P}{\rho^2} - \frac{C_p}{\beta\rho}\right)\frac{d\rho}{dt} \tag{28}$$

$$\frac{dh}{dt} = \left(\frac{\partial h}{\partial P}\right)_\rho \frac{dP}{dt} + \left(\frac{\partial h}{\partial \rho}\right)_P \frac{d\rho}{dt} = \left(\frac{1}{\rho} + \frac{C_p}{\beta\rho c_s^2}\right)\frac{dP}{dt} - \left(\frac{C_p}{\beta\rho}\right)\frac{d\rho}{dt} \tag{29}$$

$$\frac{ds}{dt} = \left(\frac{\partial s}{\partial P}\right)_\rho \frac{dP}{dt} + \left(\frac{\partial s}{\partial \rho}\right)_P \frac{d\rho}{dt} = \left(\frac{C_p}{\beta\rho T c_s^2}\right)\frac{dP}{dt} - \left(\frac{C_p}{\beta\rho T}\right)\frac{d\rho}{dt} \tag{30}$$

$$c_s^2 = \left(\frac{dP}{d\rho}\right)_s \tag{31}$$

Table 4: Selected Thermodynamic Properties Definitions

| Property | Real Fluid | Ideal Gas |
|---|---|---|
| Internal Energy | $U$ | |
| Specific Internal Energy | $de = Tds - Pdv$ | $e = \frac{P}{\rho(\gamma-1)}$ |
| Entropy | $S$ | |
| Specific Entropy | $ds = \frac{1}{T}dh - \frac{1}{T\rho}dP = \frac{1}{T}de + \frac{P}{T}dv$ | $\frac{\Delta s}{R_g} = \frac{\gamma}{\gamma-1}\ln\frac{T_2}{T_1} - \ln\frac{P_2}{P_1}$ |
| Enthalpy | $H = U + PV$ | |
| Specific Enthalpy | $h = e + Pv$ | $h = e + \frac{P}{\rho} = \frac{P}{\rho}\left(\frac{\gamma}{\gamma-1}\right)$ |
| Heat Capacity at Constant Volume | $C_v = \left(\frac{\partial U}{\partial T}\right)_V$ | |
| Specific Heat Capacity at Constant Volume | $c_v = \left(\frac{\partial e}{\partial T}\right)_v$ | |
| Heat Capacity at Constant Pressure | $C_p = \left(\frac{\partial H}{\partial T}\right)_P$ | |
| Specific Heat Capacity at Constant Pressure | $c_p = \left(\frac{\partial h}{\partial T}\right)_p$ | |
| Heat Capacity Ratio | $\frac{C_p}{C_v} = \frac{1}{1-\frac{T\beta^2}{\rho\kappa_T C_p}}$ | $\frac{C_p}{C_v} = \gamma$ |
| Isothermal Compressibility | $\kappa_T = -\frac{1}{V}\left(\frac{\partial V}{\partial P}\right)_T = \frac{1}{P} - \frac{1}{Z}\left(\frac{\partial Z}{\partial P}\right)_T = \frac{1}{\rho}\left(\frac{\partial \rho}{\partial P}\right)_T$ | $\frac{1}{P}$ |
| Isentropic Compressibility | $\kappa_s = -\frac{1}{V}\left(\frac{\partial V}{\partial P}\right)_s = \frac{1}{\rho}\left(\frac{\partial \rho}{\partial P}\right)_s = \frac{C_v}{C_p}\kappa_T$ | $\frac{1}{\gamma P}$ |
| Volume Expansion Coefficient | $\beta = \frac{1}{V}\left(\frac{\partial V}{\partial T}\right)_P = \frac{1}{T} + \frac{1}{Z}\left(\frac{\partial Z}{\partial T}\right)_P = -\frac{1}{\rho}\left(\frac{\partial \rho}{\partial T}\right)_P$ | $\frac{1}{T}$ |
| Equilibrium Speed of Sound | $c_s = \sqrt{\left(\frac{\partial P}{\partial \rho}\right)_s} = \sqrt{\frac{C_p}{C_v}\frac{1}{\kappa_T \rho}} = \sqrt{\frac{1}{\kappa_s \rho}}$ | $\sqrt{\frac{\gamma P}{\rho}}$ |
| Frozen Speed of Sound | $c_T = \sqrt{\left(\frac{\partial P}{\partial \rho}\right)_T} = \sqrt{\frac{1}{\kappa_T \rho}}$ | $\sqrt{\frac{P}{\rho}}$ |
| Isothermal Bulk Modulus of Elasticity | $E_T = \rho\left(\frac{\partial P}{\partial \rho}\right)_T = \frac{1}{\kappa_T}$ | $P$ |
| Adiabatic Bulk Modulus of Elasticity | $E_s = \rho\left(\frac{\partial P}{\partial \rho}\right)_s = \frac{C_p}{C_v}\frac{1}{\kappa_T} = \frac{C_p}{C_v}E_T$ | $\gamma P$ |
| Pressure Rise Due to Thermal Expansion | $\left(\frac{dP}{dT}\right)_V = \frac{\beta}{\kappa_T}$ | $\frac{P}{T}$ |
| Isentropic Expansion Coefficient | $\nu_s = -\frac{V}{P}\left(\frac{\partial P}{\partial V}\right)_s = \frac{1}{\kappa_T P}\frac{C_p}{C_v} = \frac{\rho}{P}c_s^2 = \frac{1}{\kappa_s P}$ | $\gamma$ |
| Joule-Thomson Coefficient | $\mu_H = \left(\frac{\partial T}{\partial P}\right)_H = -\frac{1}{C_p}\left(\frac{\partial H}{\partial P}\right)_T = \frac{1}{\rho C_p}(\beta T - 1)$ | 0 |

Additional thermodynamic properties are often used in fluid flow and pressure relief design calculations including the speed of sound, the isentropic expansion coefficient for a gas, the Joule-Thomson expansion coefficient, etc. This section provides simple and thermodynamically consistent relations for evaluation of these useful thermodynamic variables.

## 6.1 Isothermal Compressibility

The isothermal compressibility factor $\kappa_T$ is the fractional change of density with respect to pressure at constant temperature. $\kappa_T$ is typically calculated from an equation of state. The real fluid value is always larger than the ideal gas value.

$$\kappa_T = -\frac{1}{V}\left(\frac{\partial V}{\partial P}\right)_T = \frac{1}{P} - \frac{1}{Z}\left(\frac{\partial Z}{\partial P}\right)_T = \frac{1}{\rho}\left(\frac{\partial \rho}{\partial P}\right)_T \tag{32}$$

Typical values of $\kappa_T$ range from $10^{-12}$ $\mathrm{Pa}^{-1}$ to $10^{-5}$ $\mathrm{Pa}^{-1}$.

**Gases** $\kappa_T \simeq 10^{-5}$ $\mathrm{Pa}^{-1}$

**Liquids** $10^{-10} <\sim \kappa_T <\sim 10^{-9}$ $\mathrm{Pa}^{-1}$

**Solids** $10^{-12} <\sim \kappa_T <\sim 10^{-11}$ $\mathrm{Pa}^{-1}$

The isothermal compressibility factor is always larger then the adiabatic or isentropic compressibility factor. When the liquid density of pure materials is provided at saturation conditions, the isothermal compressibility factor can be used to correct the liquid density value to higher pressures:

$$\rho(T_{sat}, P) = \rho(T_{sat}, P_{sat}) + \int_{P_{sat}}^{P} \kappa_T \rho dP \tag{33}$$

or

$$\frac{\rho(T_{sat}, P)}{\rho(T_{sat}, P_{sat})} = 1.0 + \kappa_{T_{sat}} (P - P_{sat}) \tag{34}$$

Where measured speed of sound data is available for liquids, the value of the isothermal compressibility can be obtained from such measurements:

$$\kappa_T = \frac{1}{\rho c_s^2} + \frac{T\beta^2}{\rho C_P} \tag{35}$$

The second term in the above equation, $\frac{T\beta^2}{\rho C_P}$, is approximately 10 % of the total value of $\kappa_T$ for most liquids. As a result, the value of $\kappa_T$ is not very sensitive to small errors in that term.

### 6.1.1 Water Isothermal Compressibility

Several correlations appeared in the literature that allow the calculation of the isothermal compressibility for water. The correlation of Brill and Beggs is provided below as an example. This correlation does not correct for the presence of dissolved gas or solids.

$$\kappa_{T_{H_2O}} = \left(c_1 + c_2 T + c_3 T^2\right) \times 1.4507 \times 10^{-10} \ /\text{Pa} \tag{36}$$
$$c1 = 3.8546 - 1.944 \times 10^{-8} P \tag{37}$$
$$c2 = -0.01052 + 6.920 \times 10^{-11} P \tag{38}$$
$$c3 = 3.9267 \times 10^{-5} - 1.2766 \times 10^{-13} P \tag{39}$$

where P is pressure in Pascal and T is temperature in F. At 20 C (67.5 F) and 1 atmosphere (101325 Pa) this correlation yields a value of $4.819 \times 10^{-10}$ /Pa:

$$\begin{aligned} c1 &= 3.8546 - 1.944 \times 10^{-8} \times 101325 = 3.8526 \\ c2 &= -0.01052 + 6.920 \times 10^{-11} \times 101325 = -0.01051 \\ c3 &= 3.9267 \times 10^{-5} - 1.2766 \times 10^{-13} \times 101325 = 3.92541 \times 10^{-5} \\ \kappa_{T_{H_2O}} &= \left(3.8526 - 0.01051 \times 67.5 + 3.9249 \times 10^{-5} \times 67.5^2\right) \times 1.4507 \times 10^{-10} \ /\text{Pa} \\ &= 4.819 \times 10^{-10} \ /\text{Pa} \end{aligned}$$

## 6.2 Isentropic Compressibility

The isentropic compressibility factor $\kappa_s$ is the fractional change of density with respect to pressure at constant entropy. The isentropic or adiabatic compressibility factor can be calculated from the isothermal compressibility factor using the relation:

$$\kappa_s = -\frac{1}{V}\left(\frac{\partial V}{\partial P}\right)_s = \frac{1}{\rho}\left(\frac{\partial \rho}{\partial P}\right)_s = \frac{C_v}{C_p}\kappa_T \tag{40}$$

$\kappa_T$ and $\kappa_s$ are related [2]:

$$\kappa_s = \kappa_T - \frac{T}{C_p}\frac{1}{V}\left(\frac{\partial V}{\partial T}\right)_P^2 = \kappa_T\left(1 - \frac{T\beta^2}{\rho\kappa_T C_p}\right) = \kappa_T - \frac{T\beta^2}{\rho C_p} \tag{41}$$

As a result, $\kappa_T$ is always greater than $\kappa_s$.

## 6.3 Volume Expansion Coefficient

The volume expansion factor (volume expansivity) $\beta$ is equal to the change of density with respect to temperature at constant pressure:

$$\beta = \frac{1}{V}\left(\frac{\partial V}{\partial T}\right)_P = \frac{1}{T} + \frac{1}{Z}\left(\frac{\partial Z}{\partial T}\right)_P = -\frac{1}{\rho}\left(\frac{\partial \rho}{\partial T}\right)_P \tag{42}$$

[2] Note that $\left[\frac{\partial v}{\partial T}\right]_P \times \left[\frac{\partial T}{\partial P}\right]_v \times \left[\frac{\partial P}{\partial v}\right]_T = -1$ and $\frac{C_p - C_v}{T} = \left[\frac{\partial P}{\partial T}\right]_V \left[\frac{\partial v}{\partial T}\right]_P$

## 6.4 Pressure Rise Due to Thermal Expansion

This is equal to the change of pressure with respect to temperature at constant volume. It is easily expressed as the ratio of the volume expansion coefficient and isothermal compressibility:

$$\left(\frac{dP}{dT}\right)_V = \frac{\beta}{\kappa_T} \tag{43}$$

## 6.5 Isentropic Expansion Coefficient

This is expressed as a function of isothermal compressibility and heat capacity ratio:

$$\nu_s = \left[\frac{\partial \ln P}{\partial \ln V}\right]_s = -\frac{V}{P}\left(\frac{\partial P}{\partial V}\right)_s = -\frac{V}{P}\left(\frac{\partial P}{\partial V}\right)_T \frac{C_p}{C_v} = \frac{1}{\kappa_T P}\frac{C_p}{C_v} = \frac{\rho}{P}c_s^2 = \frac{1}{\kappa_s P} \tag{44}$$

For an ideal gas, $\kappa_T = 1/P$, and as a result:

$$\nu_s = \frac{C_p}{C_v} = \gamma \tag{45}$$

## 6.6 Joule-Thomson Coefficient

This is expressed in terms of the change of temperature with respect to pressure at constant enthalpy, $\mu_H$. At high pressures, negative values of $\mu_H$ indicate an increase in temperature for a constant enthalpy pressure drop. At low pressures, positive values of $\mu_H$ indicate a decrease in temperature for a constant enthalpy pressure drop.

$$\mu_H = \left(\frac{\partial T}{\partial P}\right)_H = -\frac{1}{C_p}\left(\frac{\partial H}{\partial P}\right)_T = \frac{RT^2}{PC_p}\left(\frac{\partial Z}{\partial T}\right)_P = \frac{1}{C_p}\left[T\left(\frac{\partial V}{\partial T}\right)_P - V\right] \tag{46}$$

$$= \frac{1}{\rho C_p}\left(\beta T - 1\right) \tag{47}$$

where $C_p$ is the real fluid heat capacity at constant pressure. Equation 47 can be used to construct a complete inversion curve, a curve that represents the locus of all the zero values of the Joule-Thomson coefficient. Figure 7 displays an inversion curve calculated by SuperChems using the Melhem modification of the Peng-Robinson equation of state for hydrogen. For an ideal gas, $\beta = 1/T$ and the Joule-Thomson coefficient is equal to 0. At critical conditions, it can be shown that $\mu_H$ will approach:

$$\mu_H \rightarrow \left(\frac{\partial T}{\partial P}\right)_\rho = \frac{\kappa_T}{\beta} \tag{48}$$

The inversion curve represents a severe test of the performance of an equation of state.

Figure 7: Calculated inversion curve for Hydrogen

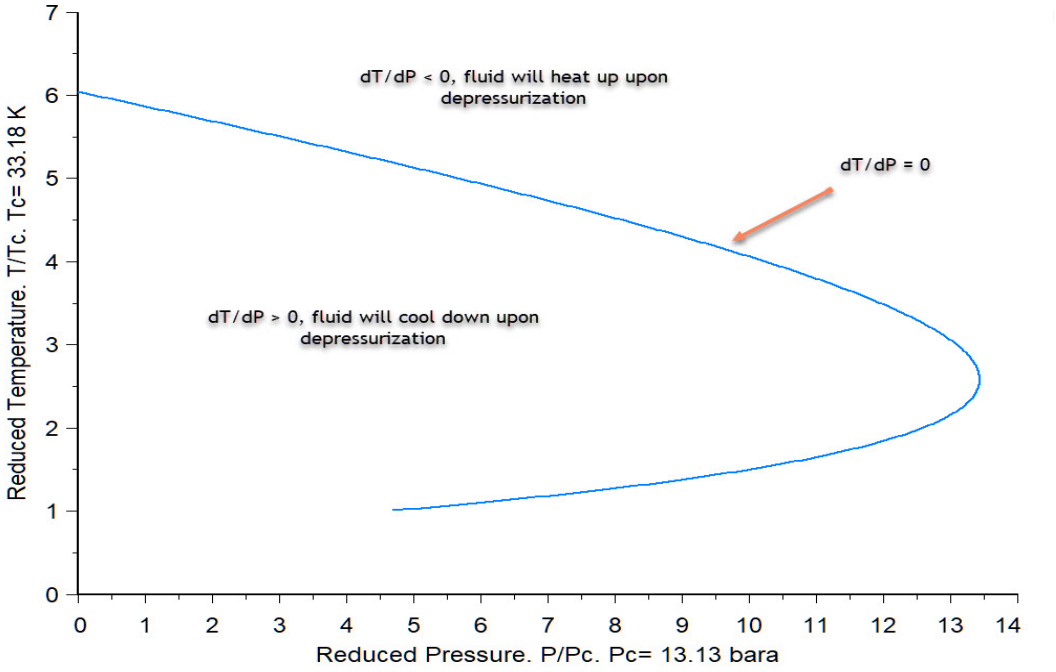


## 6.7 Liquid Constant Volume Heat Capacity

The value of liquid $C_p$ is often used as $C_v$. While this may be adequate for certain compounds, actual values of $C_v$ may be different from $C_p$ by as much as factor of two for certain chemicals such as diethyl ether, and ethyl acetate.

The value of liquid $C_v$ should be computed from an equation of state and from the liquid heat capacity at constant pressure, $C_p$:

$$C_p - C_v = T \left(\frac{\partial V}{\partial T}\right)_P \left(\frac{\partial P}{\partial T}\right)_V \tag{49}$$

or

$$C_v = C_p + \frac{T\left(\frac{\partial P}{\partial T}\right)_V^2}{\left(\frac{\partial P}{\partial V}\right)_T} = C_p - T\frac{\beta^2}{\rho\kappa_T} \tag{50}$$

$$\frac{C_p}{C_v} = \frac{\kappa_T}{\kappa_s} = \frac{1}{1 - T\frac{\beta^2}{C_p \rho \kappa_T}} \tag{51}$$

For some liquids, the heat capacity ratio can be as large as 1.5. The same relationship applies to a

real gas as well. For an ideal gas the form reduces to the well known form $C_p - C_v = R_g$:

$$\begin{aligned} \kappa_T &= \frac{1}{P} \\ \beta &= \frac{1}{T} \\ P &= \rho R_g T \\ C_p - C_v &= T\frac{\beta^2}{\rho\kappa_T} = R_g\frac{T}{T} = R_g \\ \frac{C_p}{C_v} &= \frac{\kappa_T}{\kappa_s} = \gamma \end{aligned}$$

To illustrate the impact of isothermal compressibility of the value of the heat capacity ratio for liquids, we consider the special cases of water and acetone at 20 C and 1 atmosphere.

### 6.7.1 Water Liquid Heat Capacity Ratio

$\kappa_T = 4.591 \times 10^{-10}$ /Pa, $\beta = 0.206 \times 10^{-3}$ /K, $C_p = 4184$ J/kg/K, and $\rho = 1000$ kg/m$^3$.

$$C_p - C_v = \frac{293 \times (0.206 \times 10^{-3})^2}{1000 \times 4.591 \times 10^{-10}} = 27.08 \ \text{J/kg/K} \tag{52}$$

and

$$\frac{C_p}{C_v} = \frac{4184}{4184 - 27.08} = 1.0065 \simeq 1 \tag{53}$$

As a result the equilibrium and isothermal speed of sounds for water are equal:

$$c_{S_{H_2O}} = c_{T_{H_2O}} = \sqrt{\frac{C_p}{C_v}\frac{1}{\rho\kappa_T}} = \sqrt{1.0 \times \frac{1}{1000 \times 4.591 \times 10^{-10}}} = 1476 \ \text{m/s} \tag{54}$$

### 6.7.2 Acetone Liquid Heat Capacity Ratio

$\kappa_T = 12.62 \times 10^{-10}$ /Pa, $\beta = 1.46 \times 10^{-3}$ /K, $C_p = 2167$ J/kg/K, and $\rho = 790$ kg/m$^3$.

$$C_p - C_v = \frac{293 \times (1.46 \times 10^{-3})^2}{1000 \times 12.62 \times 10^{-10}} = 626.45 \ \text{J/kg/K} \tag{55}$$

and

$$\frac{C_p}{C_v} = \frac{2167}{2167 - 626.45} = 1.4066 \tag{56}$$

As a result the equilibrium and isothermal speed of sounds for acetone are different:

$$c_{S_{C_3H_6O}} = \sqrt{\frac{C_p}{C_v}\frac{1}{\rho\kappa_T}} = \sqrt{1.4066 \times \frac{1}{790 \times 12.63 \times 10^{-10}}} = 1187.8 \text{ m/s} \tag{57}$$

$$c_{T_{C_3H_6O}} = \sqrt{\frac{1}{\rho\kappa_T}} = \sqrt{\frac{1}{790 \times 12.63 \times 10^{-10}}} = 1001.5 \text{ m/s} \tag{58}$$

## 6.8 Bulk Modulus of Elasticity

This is another common method of expressing how compressible a substance is, especially for liquids and solids. The modulus of elasticity, $E$, has units of pressure. If the compression is isothermal, the modulus of elasticity, $E_T$, can be expressed as:

$$E_T = \rho\left[\frac{\partial P}{\partial \rho}\right]_T = \frac{1}{\kappa_T} \tag{59}$$

If the compression is adiabatic, the modulus of elasticity, $E_s$, can be expressed as:

$$E_s = \rho\left[\frac{\partial P}{\partial \rho}\right]_s = \frac{C_p}{C_v}\frac{1}{\kappa_T} = \frac{C_p}{C_v}E_T \tag{60}$$

For a solid, the heat capacity ratio is approximately one. As a result, $E_s$ and $E_T$ are approximately equal for a solid:

$$E_{S,solid} \simeq E_{T,solid} = \frac{1}{\kappa_T} \tag{61}$$

As a result the speed of sound for solids can be approximated by the following expression:

$$c_{solid} \simeq \sqrt{\frac{E_{T,solid}}{\rho}} \tag{62}$$

For a non-ideal fluid, $E_s$ can also be related to the volume expansion coefficient $\beta$ and the Joule-Thomson coefficient $\mu_H$:

$$E_{S,fluid} = \frac{1}{\kappa_T - \frac{T\beta^2}{\rho C_p}} = \frac{1}{\kappa_T - \beta\left[\mu_H - 1\right]} = \frac{1}{\kappa_T - \beta\left[\left(\frac{\partial T}{\partial P}\right)_H - 1\right]} \tag{63}$$

For an ideal gas, $E_T = P$, and $E_s = \gamma P$.

### 6.8.1 Speed of Sound in Carbon Steel

The modulus of elasticity of typical carbon steel is 29000 psi or $2 \times 10^{11}$ Pa. Given a density of 7800 $\text{kg/m}^3$ the speed of sound in carbon steel is calculated to be 5063 m/s:

$$c_s \simeq c_T = \sqrt{\frac{2 \times 10^{11}}{7800}} = 5063 \text{ m/s} \tag{64}$$

Table 5: Speed of Sound Estimates vs. Measured Data in m/s at 283 K

| P, bara | Measured | Calculated. Composition 1 | Calculated. Composition 2 |
|---|---|---|---|
| 32 | 391 | 391.47 | 387.60 |
| 66 | 386 | 383.54 | 378.69 |
| 89 | 390 | 387.36 | 382.46 |
| 111 | 400 | 398.66 | 394.43 |
| 117 | 402 | 402.94 | 398.99 |
| 120 | 403 | 405.25 | 401.46 |

# 7 Validation Data

## 7.1 Gases

Measured speed of sound values were compared to SuperChems predictions for gas, liquid, and two phase mixtures. The Melhem modified Peng-Robinson equation of state as implemented in SuperChems performs very well vs. the measured data.

Table 5 summarizes predictions vs. measurements [7] for a natural gas pipeline under different pressures at 283 K. The predictions based on the provided two gas compositions are in excellent agreement with the measured data. This is especially interesting considering the depression is speed of sound measured at 66 bara which is also predicted by SuperChems. The measurements were conducted in a large scale test facility with a 48 inch pipeline that is 535 meters long. Two compositions of natural gas were provided for the gas used in the flow measurements:

**Gas 1** $N_2$ 2.2 %, $CH_4$ 88.7 %, $CO_2$ 1.24 %, $C_2$ 6.2 %, $C_3$ 1.3 %, $iC_4$ 0.13 %, $n-C_4$ 0.19 %, $iC_5$ 0.038 %, $nC_5$ 0.033 %, and $nC_6$ 0.008 %.

**Gas 2** $N_2$ 0.85 %, $CH_4$ 87.5 %, $CO_2$ 1.96 %, $C_2$ 8.34 %, $C_3$ 1.16 %, $iC_4$ 0.075 %, $n-C_4$ 0.093 %, $iC_5$ 0.014 %, and $nC_5$ 0.013 %.

Speed of sound predictions for gas and vapor systems are the most accurate using equations of states as shown above. Gas speed of sound values can be obtained with high accuracy, typically within +/- 5 % even when close to the two-phase boundaries.

## 7.2 Liquids

The literature is full of reported measurements for liquid speed of sound for pure chemicals and mixtures of chemicals. Speed of sound measurements for liquid hydrocarbons and oils were obtained from the literature and compared against the predictions of SuperChems and the Melhem modification of the Peng-Robinson cubic equation of state. The predicted values of speed of sound in hydrocarbon liquids are in good agreement with measured values (see [8]) for both pure components and mixtures including the following trends:

Figure 8: Calculated vs. Measured Liquid Speed of Sound Data for n-alkanes at 1 atm

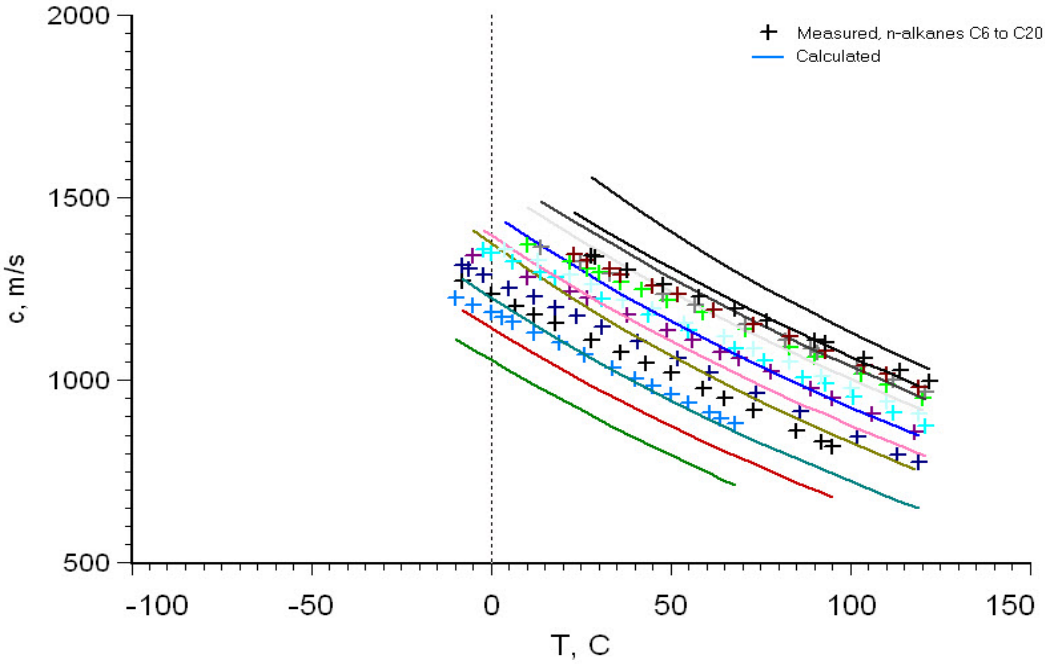


- The liquid speed of sound decreases approximately linearly with increasing temperature and increases with increasing pressure.
- The speed of sound for liquid mixtures also varies approximately linearly with temperature and liquid volume fraction.
- The speed of sound for liquid hydrocarbons increases rapidly with increasing carbon number up to C16 and then the increase becomes less sensitive to the increasing carbon number.
- The speed of sound for liquid hydrocarbons (alkanes and alkenes) is approximately a linear function of the inverse of molecular weight.

The hydrocarbon liquid speed of sound data was obtained by Wang [8]. Figures 8, 9, and 10 illustrate the predictions of SuperChems vs. the actual measured data for normal alkanes, alkenes, and cycloalkanes. The prediction errors are shown in Figure 11. The liquid speed of sound calculated by SuperChems is the isentropic liquid speed of sound. The error bounds of +/- 20 % are reasonable error bounds to use when evaluating PRV stability for liquid hydrocarbon systems.

The calculation of liquid speed of sound is a very stringent test of an equation of state's ability to predict liquid density, liquid isothermal compressibility, and the liquid heat capacity ratio. Most equations of state will not be able to calculate accurate values for liquid water for example. Cubic equations of state such as the one used in SuperChems use liquid volume translation correction for the liquid density and isothermal compressibility. As of this writing, the liquid volume translation corrections have not been applied to the departure functions of enthalpy and internal energy which may have a strong impact on the liquid heat capacity ratio. Liquid speed of sound predictions will be more accurate for liquids where the equation of state calculated liquid heat capacity ratio

Figure 9: Calculated vs. Measured Liquid Speed of Sound Data for 1-alkenes at 1 atm

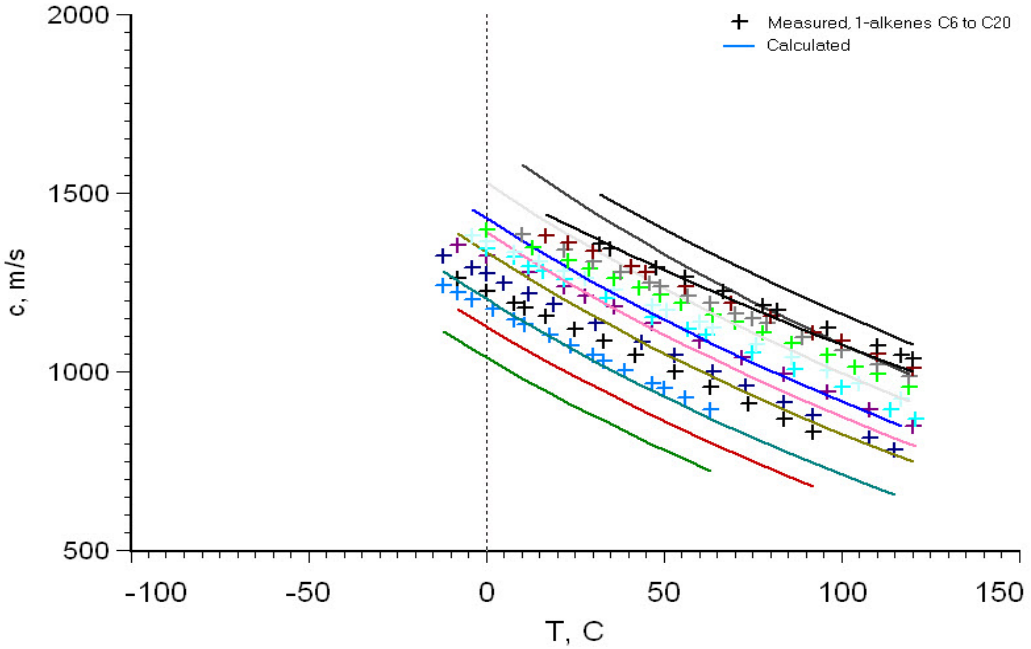


Figure 10: Calculated vs. Measured Liquid Speed of Sound Data for cycloalkanes at 1 atm

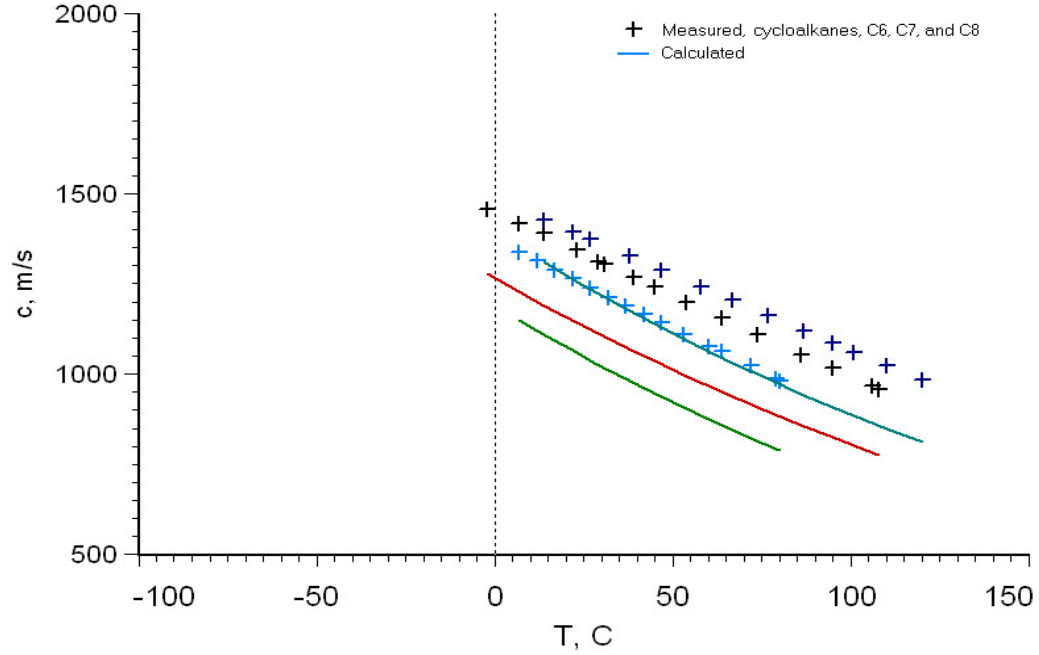

Figure 11: Predicted Error Bounds for Liquid Speed of Sound for Hydrocarbons using SuperChems

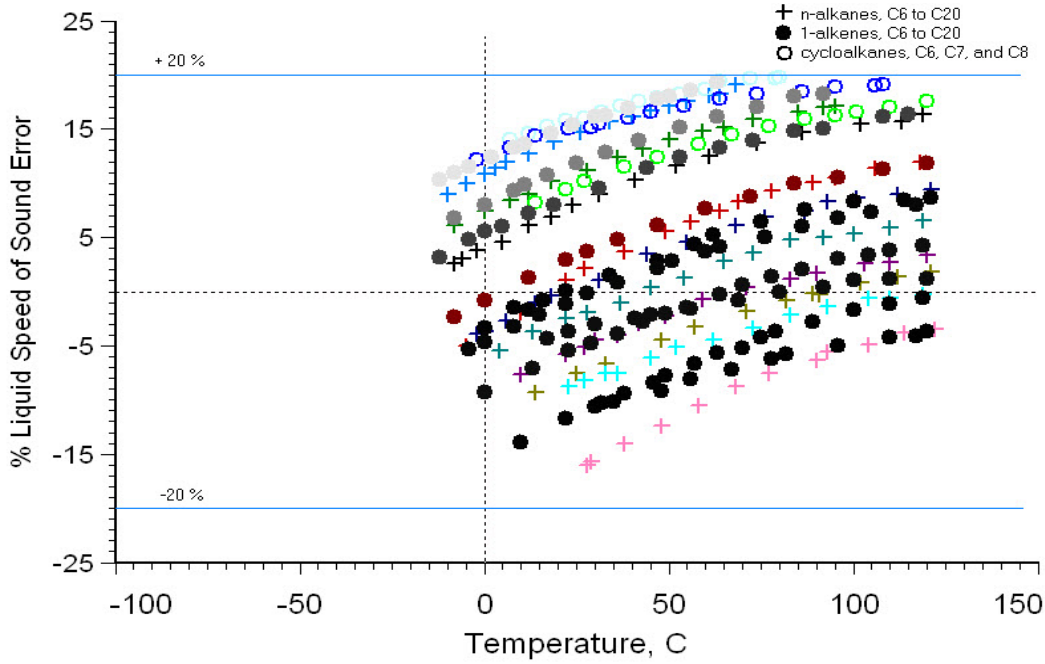


is accurate and typically close to 1. Validation of equation of state predictions for liquid speed of sound is required before use in critical applications such as PRV stability engineering analysis. This validation data can easily be obtained using laboratory measurement of liquid density and speed of sound data at different temperatures. Such measurements are available from ioKinetic testing laboratories.

### 7.3 Two-Phase

Because of the strong influence of the gas compressibility on two-phase systems, predictions of two-phase speed of sound data for most mixtures, including mixtures containing water, can be obtained well within the +/- 20 % error bounds suggested for any analysis using speed of sound data.

## 8 Conclusions

The speed of sound and associated thermodynamic properties can be accurately estimated for a wide range of fluids using SuperChems. Care must be exercised with highly incompressible liquids and two phase mixtures where the speed of sound strongly depends on the presence of small amounts of dissolved gas and/or suspended solids. Validation of liquid speed of sound data with laboratory measurement of actual plant liquid samples is highly recommended.

# 9 Appendix A - Ideal Gas Behavior

Even with high speed computing and the availability of many useful and accurate equations of state, many engineers still use a constant $\gamma$ ideal gas equation of state. This is used for example in calculating the hydraulics of flare headers at low pressure and one dimensional gas flow dynamics. A constant value of $\gamma$ is used to define the equation of state and all the associated thermodynamic properties:

$$\gamma = \frac{C_p}{C_v} = \frac{C_p}{C_p - R_g} \tag{65}$$

or

$$C_p = R_g \frac{\gamma}{\gamma - 1} \text{ or } c_p = \frac{R_g}{M_w} \frac{\gamma}{\gamma - 1} \tag{66}$$

The pressure, specific enthalpy, and specific internal energy can be calculated using the following expressions:

$$P = \rho e (\gamma - 1) = \frac{\rho R_g T}{M_w} \tag{67}$$

$$e = \frac{P}{\rho (\gamma - 1)} = \frac{R_g T}{M_w (\gamma - 1)} = \frac{c_s^2}{\gamma (\gamma - 1)} \tag{68}$$

$$h = e + \frac{P}{\rho} = \frac{P}{\rho} \left( \frac{\gamma}{\gamma - 1} \right) = \frac{R_g T}{M_w} \left( \frac{\gamma}{\gamma - 1} \right) = \frac{c_s^2}{(\gamma - 1)} \tag{69}$$

where $e$ and $h$ are internal energy and enthalpy per unit mass. It can be shown that the speed of sound in a constant flow area pipe under adiabatic conditions is equal to:

$$c_s^2 = \frac{\gamma R_g T}{M_w} = \left[ \frac{\partial P}{\partial \rho} \right]_s = \frac{1}{\rho \kappa_s} \tag{70}$$

This yields a simple expression for $\kappa_s$:

$$\kappa_s = \frac{1}{\gamma P} = \frac{\kappa_T}{\gamma} \tag{71}$$

It can also be shown that for sonic flow to occur in a constant flow area pipe under isothermal conditions, the speed of sound is equal to:

$$c_T^2 = \frac{R_g T}{M_w} = \left[ \frac{\partial P}{\partial \rho} \right]_T = \frac{1}{\rho \kappa_T} \tag{72}$$

For an ideal gas undergoing an reversible adiabatic process (isentropic compression or expansion), the initial and final state densities are correlated as follows:

$$\frac{P}{\rho^\gamma} = \text{constant} = \frac{P_1}{\rho_1^\gamma} = \frac{P_2}{\rho_2^\gamma} \tag{73}$$

or

$$\frac{P_2}{P_1} = \left( \frac{\rho_2}{\rho_1} \right)^\gamma = \left( \frac{T_2}{T_1} \right)^{\frac{\gamma}{\gamma - 1}} \tag{74}$$

For isentropic flow of an ideal gas through a nozzle, the choked pressure and temperature ratios can be calculated as follows:

$$\frac{T_2}{T_1} = \left[\frac{P_2}{P_1}\right]^{\frac{\gamma-1}{\gamma}} = \frac{2}{\gamma+1} \tag{75}$$

or

$$\frac{P_2}{P_1} = \left[\frac{2}{\gamma+1}\right]^{\frac{\gamma}{\gamma-1}} \tag{76}$$

# 10 Appendix B - Thermodynamics of Sonic Flow

Consider the steady-state adiabatic flow of a fluid in a horizontal pipe of constant cross sectional area. Neglecting work and potential energy changes, the first law of thermodynamics for an open system is written as follows:

$$\frac{1}{M_w} d\underline{H} = -u du \tag{77}$$

For a constant mass flow rate and a cross-sectional area, $du$ can be replaced by:

$$du = -u \frac{d\underline{V}}{\underline{V}} \tag{78}$$

Equation 77 becomes:

$$\frac{1}{M_w} d\underline{H} = -\frac{u^2 d\underline{V}}{\underline{V}} = \frac{1}{M_w} [T d\underline{S} + \underline{V} dP] \tag{79}$$

or

$$\frac{1}{M_w} T d\underline{S} = \underbrace{-\frac{u^2 d\underline{V}}{\underline{V}}}_{\text{negative}} \underbrace{-\frac{1}{M_w} \underline{V} dP}_{\text{positive}} \tag{80}$$

As the fluid flows in the direction of decreasing pressure, its specific volume increases, as does its velocity according to law of conservation of mass. In the direction of increasing velocity, the pressure change is negative and the volume change is positive. The contributions made to Equation 80 are opposite in direction.

To satisfy the second law of thermodynamics, entropy changes must always be positive, with a limiting value of zero. For a differential length of pipe, maximum velocity (speed of sound) is reached when $d\underline{S} = 0$. An expression for maximum velocity is obtained from Equation 80:

$$\frac{1}{c_s^2} = -\frac{M_w}{\underline{V}^2} \left( \frac{\partial \underline{V}}{\partial P} \right)_s = \left( \frac{\partial \rho}{\partial P} \right)_s \tag{81}$$

$$c_s = \sqrt{\left( \frac{\partial P}{\partial \rho} \right)_s} \tag{82}$$

Given an adequate PVT equation of state, $\frac{\partial \underline{V}}{\partial P}$ or $\frac{\partial \rho}{\partial P}$ at constant entropy can be calculated for mixtures of gases or liquids. The volume derivative with respect to pressure is re-written using thermodynamic relations as a function of ideal gas heat capacity and volumetric changes with respect to temperature and pressure:

$$\left[ \frac{\partial \underline{V}}{\partial P} \right]_s = \frac{\left( \frac{\partial \underline{V}}{\partial T} \right)_P^2 + \frac{C_p}{T} \left( \frac{\partial \underline{V}}{\partial P} \right)_T}{\frac{C_p}{T}} \tag{83}$$

The volume derivatives are readily expressed in terms of isothermal compressibility, $\kappa$, and volume

expansivity, $\beta$:

$$\beta = \frac{1}{V}\left(\frac{\partial V}{\partial T}\right)_P = \frac{1}{T} + \frac{1}{Z}\left(\frac{\partial Z}{\partial T}\right)_P \tag{84}$$

$$\kappa = -\frac{1}{V}\left(\frac{\partial V}{\partial P}\right)_T = \frac{1}{P} - \frac{1}{Z}\left(\frac{\partial Z}{\partial P}\right)_T \tag{85}$$

$\kappa$ and $\beta$ values for real fluids are always larger than $\kappa$ and $\beta$ values for an ideal fluid. Direct substitution of $\kappa$ and $\beta$ into the maximum velocity equation yields the following relation for determining the sonic velocity of a multicomponent mixture:

$$\frac{1}{c_s^2} = M_w\left[\frac{P\kappa}{ZR_gT} - \frac{\beta^2 T}{C_p}\right] \tag{86}$$

The compressibility factor and its derivative are calculated from the equation of state presented in Appendix A for liquid and vapor mixtures. For an ideal gas, Equation 86 reduces to:

$$\frac{1}{c_s^2} = \frac{M_w}{R_gT}\left[1 - \frac{R_g}{C_p}\right] \tag{87}$$

The term $R_g/C_p$ can be evaluated as a function of the heat capacity ratio for an ideal gas:

$$\frac{1}{c_s^2} = \frac{M_w}{R_gT}\left[\frac{1}{\gamma}\right] \tag{88}$$

or

$$c_s = \sqrt{\frac{\gamma R_g T}{M_w}} \tag{89}$$

For an ideal gas, the speed of sound is a function of temperature only.

# References

[1] Csaba Hos. Effect of lift restriction and multicomponent flow on prv stability. In *Joint US DIERS and European Diers Users Group (EDUG)*. DIERS/EDUG, September 2023.

[2] John D. Desain and Brian B. Brady. Thermal conductivity and speed of sound measurements of liquid hydrazine (N2H4) at 293.15K and 0.101 MPa to 2.068 MPa. Technical Report TR-2008(8565)-5, The Aerospace Corporation, 2003.

[3] G. B. Wallis. *One-Dimensional Two-Phase Flow*. McGraw-Hill Book Company, New York, 1st edition, 1969.

[4] Henry R. E., M. A. Grolmes, and H. K. Fauske. Pressure pulse propagation in two-phase one- and two-component mixtures. Technical Report 7792, Argonne National Laboratory, 1971.

[5] C. J. Hos, A. R. Champneys, K. Paul, and M. McNeely. Dynamic behavior of direct spring loaded pressure relief valves: III valves in liquid service. *Journal of Loss Prevention in the Process Industries*, 43:1–9, 2016.

[6] G. A. Melhem. PRV stability inlet line critical length. A short communication. *ioMosaic Corporation White Paper*, March 2021.

[7] G. Bernasconi, S. Del Giudice, Politecnico di Milano G. Giunta, and F. Dionigi. Advanced pipeline monitoring using multipoint acoustic data. In *11th Offshore Mediterranean Conference and Exhibition, Ravenna, Italy*, 2013.

[8] Z. Wang. *Wave Velocities in Hydrocarbons and Hydrocarbons Saturated Rocks - with Applications to EOR Monitoring*. PhD thesis, Stanford University, 1988.

....

# Index

Chemical reactivity, 34

Dust, 34

Flammability, 34

ioKinetic® , 34
ioMosaic® , 33, 34
ISO certified, 34

# About the Authors

Dr. Melhem is an internationally known pressure relief and flare systems, chemical reaction systems, process safety, and risk analysis expert. In this regard he has provided consulting, design services, expert testimony, incident investigation, and incident reconstruction for a large number of clients. Since 1988, he has conducted and participated in numerous studies focused on the risks associated with process industries fixed facilities, facility siting, business interruption, and transportation.

Prior to founding ioMosaic® Corporation, Dr. Melhem was president of Pyxsys Corporation; a technology subsidiary of Arthur D. Little Inc. Prior to Pyxsys and during his twelve years tenure at Arthur D. Little, Dr. Melhem was a vice president of Arthur D. Little and managing director of its Global Safety and Risk Management Practice and Process Safety and Reaction Engineering Laboratories.

Dr. Melhem holds a Ph.D. and an M.S. in Chemical Engineering, as well as a B.S. in Chemical Engineering with a minor in Industrial Engineering, all from Northeastern University. In addition, he has completed executive training in the areas of Finance and Strategic Sales Management at the Harvard Business School. Dr. Melhem is a Fellow of the American Institute of Chemical Engineers (AIChE) and Vice Chair of the AIChE Design Institute for Emergency Relief Systems (DiERS).

### Contact Information

Georges. A. Melhem, Ph.D., FAIChE
E-mail. melhem@iomosaic.com

ioMosaic Corporation
93 Stiles Road
Salem, New Hampshire 03079
Tel. 603.893.7009, x 1001
Fax. 603.251.8384
web. www.iomosaic.com

# How can we help?

Please visit www.iomosaic.com and www.iokinetic.com to preview numerous publications on process safety management, chemical reactivity and dust hazards characterization, safety moments, video papers, software solutions, and online training.

In addition to our deep experience in process safety management (PSM), chemical reaction systems, and the conduct of large-scale site wide relief systems evaluations by both static and dynamic methods, we understand the many non-technical and subtle aspects of regulatory compliance and legal requirements. When you work with ioMosaic® you have a trusted ISO certified partner that you can rely on for assistance and support with the lifecycle costs of relief systems to achieve optimal risk reduction and PSM compliance that you can evergreen. We invite you to connect the dots with ioMosaic®.

We also offer laboratory testing services through ioKinetic® for the characterization of chemical reactivity and dust/flammability hazards. ioKinetic® is an ISO accredited, ultramodern testing facility that can assist in minimizing operational risks. Our experienced professionals will help you define what you need, conduct the testing, interpret the data, and conduct detailed analysis. All with the goal of helping you identify your hazards, define and control your risk.

ioMosaic®
Minimizing risk. Maximizing potential.®

## About ioMosaic Corporation

Our mission is to help you protect your people, plant, stakeholder value, and our planet.

Through innovation and dedication to continual improvement, ioMosaic has become a leading provider of integrated process safety and risk management solutions. ioMosaic has expertise in a wide variety of disciplines, including pressure relief systems design, process safety management, expert litigation support, laboratory services, training, and software development.

As a certified ISO 9001:2015 Quality Management System (QMS) company, ioMosaic offers integrated process safety and risk management services to help you manage and reduce episodic risk. Because when safety, efficiency, and compliance are improved, you can sleep better at night. Our extensive expertise allows us the flexibility, resources, and capabilities to determine what you need to reduce and manage episodic risk, maintain compliance, and prevent injuries and catastrophic incidents.

## Consulting Services

- Asset Integrity
- Auditing
- Due Diligence
- Facility Siting
- Fault Tree/SIL Analysis
- Fire & Explosion Dynamics
- Incident Investigation, Litigation Support, and Expert Testimony
- Hydrogen Safety
- LNG Safety
- LPG Safety
- Pipeline Safety
- Process Hazard Analysis
- Process Engineering Design and Support
- Process Safety Management
- Relief and Flare Systems Design and Evaluation
- Risk Management Program Development
- Quantitative Risk Assessment
- Software Solutions
- Structural Dynamics
- Sustainability Reporting Support
- Technology Transfer Package Development
- Process Safety Training

## Laboratory Testing Services (ISO Accredited)

- Battery Safety Testing
- Chemical Reactivity Testing
- Combustible Dust Hazard Analysis and Testing
- Flammability Testing
- Physical Properties Testing
- Process Safety Services
- Specialized Testing

## US Offices

Salem, New Hampshire
Houston, Texas
Minneapolis, Minnesota
Berkeley, California

## International Offices

Al Seef, Kingdom of Bahrain
Bath, United Kingdom

## Software Solutions

Process Safety Office® : A suite of integrated tools for process safety professionals and risk analysts.

Process Safety Enterprise® : Process Safety Management compliance made easy with enterprise workflows, dynamic forms, document management, key performance indicators and metrics, and more.

Process Safety Learning® : Build your process safety competencies incrementally using learning modules.

Process Safety tv® : The worldś first video streaming platform dedicated to process safety.

## Contact us

www.ioMosaic.com
sales@ioMosaic.com
1.844.ioMosaic